

Acetylcholinesterase Choline-Based Ionic Liquid Inhibitors: In Vitro and in Silico Molecular Docking Studies

Filipa Siopa,^{*,†} Raquel F. M. Frade,[†] Ana Diniz,[‡] Joana M. Andrade,[§] Marisa Nicolai,[§] Ana Meirinhos,[†] Susana D. Lucas,[†] Filipa Marcelo,[‡] Carlos A. M. Afonso,[†] and Patrícia Rijo^{*,†,§}

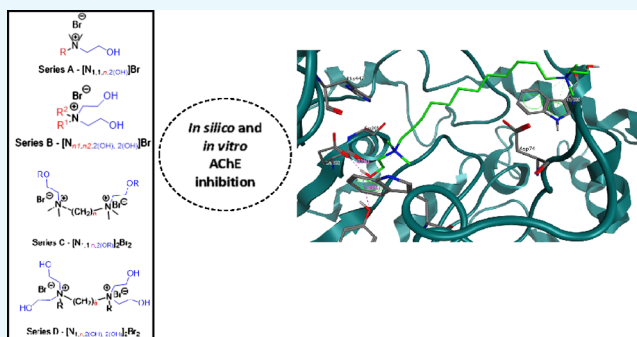
[†]Research Institute for Medicines (iMed.Ulisboa), Faculty of Pharmacy, Universidade de Lisboa, Av. Prof. Gama Pinto, 1649-003 Lisboa, Portugal

[‡]UCIBIO, REQUIMTE, Departamento de Química, Faculdade de Ciências e Tecnologia, Universidade de Nova de Lisboa, 2829-516 Caparica, Portugal

[§]Research Center for Biosciences & Health Technologies (CBIOS), Universidade Lusófona de Humanidades e Tecnologias, Campo Grande 376, 1749-024 Lisboa, Portugal

Supporting Information

ABSTRACT: Monocationic and dicationic cholinium ionic liquids (ILs) were synthesized and evaluated as acetylcholinesterase (AChE) inhibitors with in vitro and in silico models, and their cytotoxicity was assessed using human cell lines from skin (CRL-1502) and colon cancer (CaCo-2). The ILs with a longer alkyl chain were stronger AChE inhibitors, the dicationic ILs (DILs) being more active than the monocationic ILs. The best result was obtained for $[N_{1,1,12,2}(\text{OH})_2]\text{Br}_2$ at a concentration of $0.18 \mu\text{M}$ by reducing half enzyme activity without affecting the viability of tested cell lines. A saturation-transfer difference NMR (STD-NMR) binding study was carried out, demonstrating that $[N_{1,1,12,2}(\text{OH})_2]\text{Br}_2$ binds to AChE. STD-NMR competition binding experiments, using galanthamine as a reference ligand, clearly highlight that the IL displaces galanthamine in the AChE binding site pinpointing $[N_{1,1,12,2}(\text{OH})_2]\text{Br}_2$ inside the deep gorge of AChE. In order to obtain a three-dimensional (3D) view of the molecular recognition process, in silico molecular docking studies on the active site of AChE were carried out. The proposed 3D model of the AChE/DIL complex is in agreement with the STD-derived epitope mapping, which explains the competition with galanthamine and unveils key interactions in both peripheral and catalytic sites of AChE. These interactions seem essential to govern the recognition of DILs by the AChE enzyme. Our study provides a structural and functional platform that can be used for the rational design of choline-based ILs as potent AChE inhibitors.



1. INTRODUCTION

Acetylcholinesterase (AChE) is a member of the α/β hydrolase protein super family, which catalyzes the hydrolysis of acetylcholine (ACh) in the cholinergic synapses.^{1–4} In the peripheral nervous system, ACh mediates nerve impulse in neuromuscular junctions and is a major neurotransmitter in the autonomic nervous system controlling memory and learning processes.⁵ There has been a growing interest in AChE because of its importance in neurodegenerative diseases such as Alzheimer's disease (AD). A deficiency in ACh is linked to the pathogenesis of AD, resulting in a decline in memory and recognition.^{6–9}

AChE contains various binding domains—catalytic, anionic, acyclic, oxyanionic, and peripheral anionic. The first domain is situated at the bottom of 20 Å deep and narrow binding gorge and contains the catalytic triad composed by Ser203, Glu334, and His447. The anionic domain is formed by four aromatic residues—Trp86, Tyr130, Tyr337, and Phe338 and is the

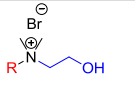
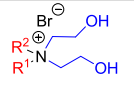
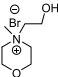
binding site for the quaternary trimethylammonium choline moiety. The acyl domain is constituted by two bulky residues—Phe295 and Phe297 that are responsible for the selective binding of ACh. The oxyanionic hole is formed by Gly121, Gly122, and Ala204 and hosts one molecule of structural water, which is responsible for the formation of a hydrogen bond between the enzyme and substrate stabilizing the substrate tetrahedral transition state. The peripheral anionic site (PAS) is one of the most important drug target binding sites and is located at the entrance to the binding gorge presenting five residues—Tyr72, Asp74, Tyr124, Trp286, and Tyr341. PAS participates in noncholinergic functions as amyloid deposition, and therefore, inhibitors

Received: September 11, 2018

Accepted: November 29, 2018

Published: December 12, 2018

Table 1. Mono-Quaternary Ammonium Salt Choline Derivatives (Series A–B)

 Series A - $[N_{1,1,n,2(OH)}]Br$			 Series B - $[N_{n1,n2,2(OH),2(OH)}]Br$			
Compound	n	R	Compound	n1,n2	R ¹	R ²
$[N_{1,1,2,2(OH)}]Br$	2	C ₂ H ₅	$[N_{0,3,2(OH),2(OH)}]Br$	0,3	H	C ₃ H ₇
$[N_{1,1,3,2(OH)}]Br$	3	C ₃ H ₇	$[N_{0,12,2(OH),2(OH)}]Br$	0,12	H	C ₁₂ H ₂₅
$[N_{1,1,4,2(OH)}]Br$	4	C ₄ H ₉	$[N_{0,14,2(OH),2(OH)}]Br$	0,14	H	C ₁₄ H ₂₉
$[N_{1,1,5,2(OH)}]Br$	5	C ₅ H ₁₁	$[N_{0,16,2(OH),2(OH)}]Br$	0,16	H	C ₁₆ H ₃₃
$[N_{1,1,6,2(OH)}]Br$	6	C ₆ H ₁₃	$[N_{1,3,2(OH),2(OH)}]Br$	1,3	CH ₃	C ₃ H ₇
$[N_{1,1,8,2(OH)}]Br$	8	C ₈ H ₁₇	$[N_{1,4,2(OH),2(OH)}]Br$	1,4	CH ₃	C ₄ H ₉
$[N_{1,1,10,2(OH)}]Br$	10	C ₁₀ H ₂₁	$[N_{1,6,2(OH),2(OH)}]Br$	1,6	CH ₃	C ₆ H ₁₃
$[N_{1,1,12,2(OH)}]Br$	12	C ₁₂ H ₂₅	$[N_{1,10,2(OH),2(OH)}]Br$	1,10	CH ₃	C ₁₀ H ₂₁
$[N_{1,1,14,2(OH)}]Br$	14	C ₁₄ H ₂₉	$[N_{1,12,2(OH),2(OH)}]Br$	1,12	CH ₃	C ₁₂ H ₂₅
$[N_{1,1,16,2(OH)}]Br$	16	C ₁₆ H ₃₃	$[N_{1,14,2(OH),2(OH)}]Br$	1,14	CH ₃	C ₁₄ H ₂₉
$[N_{1,1,3=,2(OH)}]Br$	3=	CH ₂ CH=CH ₂	$[N_{1,3=,2(OH),2(OH)}]Br$	1,3=	CH ₃	CH ₂ CH=CH ₂
$[N_{1,1,6=,2(OH)}]Br$	6=	(CH ₂) ₄ CH=CH ₂	$[N_{1,6=,2(OH),2(OH)}]Br$	1,6=	CH ₃	(CH ₂) ₄ CH=CH ₂
$[N_{1,1,3\equiv,2(OH)}]Br$	3≡	CH ₂ C≡CH	$[N_{3=,2(OH),2(OH),2(OH)}]Br$	3=,2(OH)	CH ₂ CH=CH ₂	CH ₂ CH ₂ OH
$[N_{1,1,Cycl,2(OH)}]Br$	cycl	(cycl)C ₆ H ₁₁	$[N_{4,2(OH),2(OH),2(OH)}]Br$	4,2(OH)	C ₄ H ₉	CH ₂ CH ₂ OH
$[N_{1,morf,2(OH)}]Br$	morf		$[N_{6,2(OH),2(OH),2(OH)}]Br$	6,2(OH)	C ₆ H ₁₃	CH ₂ CH ₂ OH

that bind to both catalytic site and PAS are crucial for AD treatment.^{4,10}

AChE inhibitors, such as rivastigmine, donepezil, tacrine, and galantamine, approved by Food and Drug Administration present some drawbacks. Tacrine induces significant liver toxicity and the others seem inefficient to block or slow down the progress of AD.^{6,8,11–14} Several new inhibitors have been documented being hybrid molecules relevant compounds on AChE inhibition.^{10,14,15}

Quaternary and bis-quaternary ammonium salts have been investigated as AChE inhibitors, which include pyridinium, quinolinium, isoquinolinium, and quinuclidinium as cations.^{5,9,11,13,16–22} Additionally, ionic liquids (ILs) have also been investigated as AChE inhibitors.^{23–28} It has been demonstrated that the potency of AChE inhibition by ILs depends on the positively charged nitrogen atom, a widely delocalized aromatic system, and the lipophilicity of the side chains connected to the cationic head groups, the last one being identified as a potent structural element for AChE inhibition.^{23,29} Stock et al. have shown that pyridinium-based ILs induced a stronger inhibition than imidazolium-based ILs.²⁴ Moreover, Arning and co-workers observed that quinolinium-based ILs together with dimethylaminopyridinium were stronger AChE inhibitors than morpholinium-based ILs.²³

The influence of dicationic ILs (DILs) on AChE activity was also addressed.²⁸ Similar to monocationic imidazolium-based ILs, increasing the side-chain length also leads to a higher inhibitory potential of the DILs.^{23,28} However, DILs are less potent inhibitors when compared to the corresponding monocationic ILs.²⁸

The search for more potent and AChE inhibitors is still ongoing, and the “greener” choline-based ILs have gained particular attention.^{30,31} We studied the impact of mono- and dicholine-based ILs with different chain lengths and chemical functionalities on AChE activity and evaluated the cytotoxicity on human cell lines from skin (CRL-1502) and intestinal cancer (CaCo-2). In addition, we report NMR spectroscopy binding studies of the DIL $[N_{1,1,12,2(OH)}]_2Br_2$ versus AChE. In particular, we have employed saturation-transfer difference NMR (STD-NMR) to evaluate the binding of DIL to AChE and to determine the binding epitope mapping. In addition, STD-NMR competition binding experiments using the well-studied inhibitor galanthamine as a reference ligand were performed to assess the DIL binding site. Finally, NMR-derived data were combined with molecular docking to obtain a 3D model of the AChE/DIL complex structure.

2. METHODS AND MATERIALS

2.1. Chemicals. All chemicals, reagents, and solvents for the synthesis of the compounds were of analytical grade, purchased from commercial sources, namely, Sigma-Aldrich, Merck, and Alfa Aesar, and were used without further purification. AChE-type VI-S, from electric eel 349 U/mg solid, 411 U/mg protein, and acetylthiocholine iodide (AChI, ≥98%) were purchased from Sigma-Aldrich. 5,5'-Dithio-bis-(2-nitrobenzoic acid) (DTNB) was purchased from VWR International Prolabo. 1,2,3,4-Tetrahydro-5-aminoacridine (Tacrine) was obtained from Cayman Chemical Company. The compounds 1,14-dibromotetradecane and 1,6-dibromohexadecane were synthesized with some modifications of the reported procedure.³² ¹H and ¹³C NMR spectra were recorded

Table 2. Range of Bis-Quaternary Ammonium Salt Choline Derivatives (Series C–D)

Series C - $[N_{1,1,n,2(OR)}]_2Br_2$			Series D - $[N_{1,n,2(OH),2(OH)}]_2Br_2$		
Compound	R	n	Compound	R	n
$[N_{1,1,12,2(OH)}]_2Br_2$	H	12	$[N_{1,8,2(OH),2(OH)}]_2Br_2$	CH ₃	8
$[N_{1,1,12,2(OCOCH_3)}]_2Br_2$	COCH ₃	12	$[N_{1,10,2(OH),2(OH)}]_2Br_2$	CH ₃	10
$[N_{1,1,14,2(OH)}]_2Br_2$	H	14	$[N_{1,12,2(OH),2(OH)}]_2Br_2$	CH ₃	12
$[N_{1,1,16,2(OH)}]_2Br_2$	H	16	$[N_{6,2(OH),2(OH)2(OH)}]_2Br_2$	CH ₂ CH ₂ OH	6
$[N_{1,1,Bn,2(OH)}]_2Br_2$	H	1Ph	$[N_{8,2(OH),2(OH)2(OH)}]_2Br_2$	CH ₂ CH ₂ OH	8
			$[N_{10,2(OH),2(OH)2(OH)}]_2Br_2$	CH ₂ CH ₂ OH	10
			$[N_{12,2(OH),2(OH)2(OH)}]_2Br_2$	CH ₂ CH ₂ OH	12
			$[N_{Bn,2(OH),2(OH)2(OH)}]_2Br_2$	CH ₂ CH ₂ OH	1Ph

on an Ultrashield Bruker AVANCE II 300 spectrometer, an Ultrashield Bruker AVANCE II 400 spectrometer, and a Bruker Fourier 300 spectrometer. Splitting patterns are indicated as s, singlet; d, doublet; t, triplet; q, quartet; m, multiplet; br, broad peak. The low-resolution electrospray ionization (ESI) mass spectra were recorded using a Micromass Quattro Micro triple quadrupole (Waters, Ireland) with an ESI ion source. High-resolution mass spectroscopy was performed in a Bruker micrOTOF mass spectrometer, with an ESI ion source, and in a LTQ Orbitrap XL mass spectrometer (Thermo Fischer Scientific, Bremen, Germany). Elemental analysis was performed in a FLASH 2000 CHNS-O analyzer (Thermo Scientific, UK). The general procedure was adopted for the samples submitted to elemental analysis, which were first kept overnight under vacuum line (rotatory pump, below 0.5 mbar) and then kept at room temperature for 3–5 days in a dedicated vacuum line (rotatory pump, below 0.2 mbar). Melting points were determined on a Stuart SMP10 apparatus.

2.1.1. General Procedure for the Preparation of Quaternary and Bis-Quaternary Ammonium Salts. The quaternary ammonium salts were synthesized by amine alkylation with the selected alkyl halide. The mono-quaternary ammonium salts from series A (Table 1) and series B (Table 1), with exception of compounds $[N_{1,1,Cycl,2(OH)}]Br$, $[N_{1,morf,2(OH)}]Br$, $[N_{0,12,2(OH),2(OH)}]Br$, and $[N_{0,16,2(OH),2(OH)}]Br$, have been previously reported by us.^{33,34} The salts $[N_{1,1,Cycl,2(OH)}]Br$, $[N_{1,morf,2(OH)}]Br$, and $[N_{0,16,2(OH),2(OH)}]Br$ were prepared with some modifications of the literature,^{35–37} and together with the new IL $[N_{0,12,2(OH),2(OH)}]Br$, they are described in detail in the Supporting Information.

The bis-quaternary ammonium salts (series C–D; Table 2) were prepared following the same strategy as the mono-quaternary ammonium salts. The synthesis and characterization of the compounds $[N_{1,8–12,2(OH),2(OH)}]_2Br_2$ and $[N_{6–12,2(OH),2(OH)2(OH)}]_2Br_2$ have been previously published by our group.³⁵ For the new bis-quaternary ammonium salts $[N_{1,1,12–16,2(OH)}]_2Br_2$, $[N_{1,1,Bn,2(OH)}]_2Br_2$, $[N_{1,1,12,2(OCOCH_3)}]_2Br_2$, and $[N_{Bn,2(OH),2(OH)2(OH)}]_2Br_2$, see more details in the Supporting Information.

Additional experimental details and selected ¹H and ¹³C NMR spectra are presented in the Supporting Information.

2.2. AChE Inhibition Assay. The AChE inhibition assay was performed by the Ellman method, as previously described,

with some modifications^{38,39} with acetylcholine iodide as a substrate and DTNB. A mixture of *N*-(2-hydroxyethyl)-piperazine-*N'*-ethanesulfonic acid buffer (50 mM, pH 8.0), sample solution (30 μL), and AChE enzyme (2.5 U/mL, 7.5 μL) was incubated in a 96-well plate for 15 min at 25 °C. The reaction was then initiated by the addition of AChI (1.20 mM, 22.5 μL) and DTNB (3.03 mM, 142 μL) (*n* = 3). The hydrolysis of acetylthiocholine was monitored, every 30 s for 3 min, by the formation of a yellow 5-thio-2-nitrobenzoate anion as a result of the reaction of DTNB with thiocholine, produced by the enzymatic hydrolysis of acetylthiocholine, at a wavelength of 405 nm, using a 96-well microplate plate reader (Multiskan FC Thermo Fisher Scientific). Tacrine was used as positive control and sample solvent as negative control.

The inhibition percentage was determined using the following equations:

$$\text{Velocity reaction of control or inhibitor} = \frac{\text{corrected absorbance 405 nm}}{\text{time (min)}} \quad (\text{a})$$

$$\text{Inhibitor activity (\%)} = 100 - \left(\frac{100 \times \text{velocity reaction of inhibitor}}{\text{velocity reaction of control}} \right) \quad (\text{b})$$

It is known that for a the velocity reaction of negative control ($\Delta Abs_{405nm}/\text{min}$) should be linear and hence close to 0.060.

2.3. Cell Culture. Human colorectal adenocarcinoma cells (CaCo-2) and human normal skin fibroblast cells (CRL-1502), purchased from the American Type Culture Collection (ATCC), were grown in RPMI-1640 medium supplemented with 10% fetal bovine serum (FBS) and antibiotic–antimycotic solution. They were kept in 75 cm² tissue culture flasks and in an incubator with a humidified 5% CO₂ atmosphere at 37 °C.

2.3.1. Toxicity Assay. A total of 96-well plates with 3–4 days of postconfluent differentiated CaCo-2 cells were treated with the ILs at 1 mM concentration for a 24 h period. Solutions were prepared with fresh 0.5% FBS supplemented medium. After the removal of compounds, cell viability was assessed with the neutral red reagent. IL-treated medium was removed, and cells were washed with phosphate buffer saline

Table 3. AChE Enzymatic Inhibition and Cytotoxicity toward Human Cell Lines^a

compound	concentration (mM)	inhibition \pm SD (100 μ g/mL)	IC ₅₀ (μ M)	CRL-1502 (1 mM)	CaCo-2 (1 mM)
[N _{1,1,2} (OH)]Br	0.505	6.92 \pm 1.83	-	NT	NT
[N _{1,1,3} (OH)]Br	0.471	52.5 \pm 2.04	-	NT	NT
[N _{1,1,4} (OH)]Br	0.442	63.8 \pm 3.65	-	NT	NT
[N _{1,1,5} (OH)]Br	0.416	16.9 \pm 3.91	-	NT	NT
[N _{1,1,6} (OH)]Br	0.393	25.6 \pm 1.63	-	NT	NT
[N _{1,1,8} (OH)]Br	0.354	49.2 \pm 0.74	-	NT	NT
[N _{1,1,10} (OH)]Br	0.322	88.7 \pm 2.99	48.5	VT	NT
[N _{1,1,12} (OH)]Br	0.296	96.4 \pm 1.98	13.8	ND	T
[N _{1,1,14} (OH)]Br	0.273	100 \pm 1.28	6.00	VT	VT
[N _{1,1,16} (OH)]Br	0.273	99.3 \pm 0.81	5.94	VT	NT
[N _{1,1,3=2} (OH)]Br	0.476	47.6 \pm 1.27	-	NT	NT
[N _{1,1,6=2} (OH)]Br	0.397	28.5 \pm 1.50	-	NT	NT
[N _{1,1,3=2} (OH)]Br	0.481	51.0 \pm 1.35	-	NT	NT
[N _{1,1,Cycl} (OH)]Br	0.397	31.5 \pm 2.62	-	NT	NT
[N _{1,morf} (OH)]Br	0.442	23.9 \pm 1.14	-	NT	NT
[N _{0,3,2} (OH) ₂ (OH)]Br	0.438	55.5 \pm 2.59	-	NT	NT
[N _{0,12,2} (OH) ₂ (OH)]Br	0.282	98.0 \pm 0.92	32.5	ND	T
[N _{0,14,2} (OH) ₂ (OH)]Br	0.261	95.9 \pm 1.46	11.3	VT	VT
[N _{0,16,2} (OH) ₂ (OH)]Br	0.244	66.3 \pm 5.26	-	ND	VT
[N _{1,3,2} (OH) ₂ (OH)]Br	0.413	31.5 \pm 2.15	-	NT	NT
[N _{1,4,2} (OH) ₂ (OH)]Br	0.390	66.0 \pm 2.18	-	NT	NT
[N _{1,6,2} (OH) ₂ (OH)]Br	0.352	7.91 \pm 1.72	-	NT	NT
[N _{1,10,2} (OH) ₂ (OH)]Br	0.294	79.6 \pm 0.48	58.9	VT	VT
[N _{1,12,2} (OH) ₂ (OH)]Br	0.271	92.2 \pm 2.67	23.9	VT	VT
[N _{1,14,2} (OH) ₂ (OH)]Br	0.252	75.1 \pm 2.16	7.87	VT	NT
[N _{1,3=2} (OH) ₂ (OH)]Br	0.416	37.4 \pm 2.09	-	NT	NT
[N _{1,6=2} (OH) ₂ (OH)]Br	0.354	19.7 \pm 1.79	-	NT	NT
[N ₃₌₂ (OH) ₂ (OH) ₂ (OH)]Br	0.370	21.2 \pm 2.77	-	NT	NT
[N _{4,2} (OH) ₂ (OH) ₂ (OH)]Br	0.349	37.1 \pm 2.37	-	NT	VT
[N _{6,2} (OH) ₂ (OH) ₂ (OH)]Br	0.318	38.1 \pm 0.62	-	ND	T
tacrine	0.05	61.9 \pm 1.88	0.021	-	-
			0.018		
donepezil	NT	NT	(0.006–0.012) ^b	-	-

^aCompounds from series A and B were tested at a single dose in each biological assay. ^bCompounds were considered NT, T, or VT when the viability decrease did not attain the IC₅₀ of the compound (less than 50%) or reached 50–80% decrease or was higher than 80%, respectively. “-” not evaluated.

(PBS) before treatment with 50 μ g/mL neutral red for 15 min. After this period, cells were washed with PBS and incubated with an organic solution (49% water, 50% ethanol, and 1% glacial acetic acid) for the quantification of absorbed neutral red dye. Dye was measured spectrophotometrically at 540 nm after gentle shaking of the plate. Viability was calculated as the ratio of the absorbance of treated and untreated cells. Each experimental condition was done in triplicate. Compounds were considered not toxic (NT), toxic (T), or very toxic (VT) when cytotoxicity was below 50, 50–80%, or was above 80%, respectively.

CRL-1502 cells were treated likewise, but compounds were added soon after the formation of the monolayer and neutral red was left in contact with these cells for a period of 3 h.

2.4. Molecular Docking. AChE 3.10 Å resolution crystallographic structure was obtained from the Protein Data Bank with code 4BDT. Prior to docking studies, the cocrystallized inhibitor and water molecules were removed. The Protonate-3D tool from Molecular Operating Environment (MOE) 2014 software package⁴⁰ was used to protonate AChE, considering His 447 basic tautomer, and then MMFF94x force field was applied for energy minimization. Molecular docking studies were performed using GOLD 5.2

software package, namely, the GoldScore scoring function in which each molecule is subjected to 2000 docking runs, at a 10 Å distance from the Trp86 N atom, was considered the active site center coordinate. To validate the above-described docking protocol of the 4BDT, the cocrystallized inhibitor, huprine W, was docked using this methodology, and the root-mean-square deviation value between docked and crystallographic poses obtained was 1.27 Å. For the molecules studied, the 10 highest gold scored docking poses were visually inspected, and both were highly superposable, the presented result (Figure 3) being the highest scored pose.

2.5. NMR Spectroscopy Experiments. NMR spectroscopy experiments were recorded on a Bruker AVANCE 600 MHz spectrometer with a 5 mm triple-resonance cryogenic probe head. All experiments were carried out at 298 K using PBS (20 mM) buffer at pH 7.5. For NMR studies, AChE was used from the eel *Electrophorus electricus* from Sigma-Aldrich, which is a tetramer composed by four equal subunits of 70 kDa each (each subunit holds one active site).

STD-NMR experiments were carried out for a protein/DIL molar ratio of 1:30 with a final concentration of 10 μ M protein and 300 μ M DIL. To confirm protein specificity, protein concentration was raised to 20 μ M by maintaining constant

Table 4. AChE Enzymatic Inhibition and Cytotoxicity toward Human Cell Lines^{a,b}

compound	concentration (mM)	inhibition \pm SD (100 μ g/mL)	IC ₅₀ (μ M)	CRL-1502 (1 mM)	CaCo-2 (1 mM)
[N _{1,1,12,2(OH)}] ₂ Br ₂	0.198	100 \pm 0.72	0.18	ND	NT
[N _{1,1,12,2(OCHOCH₃)}] ₂ Br ₂	0.182	100 \pm 0.15	0.42	ND	NT
[N _{1,1,14,2(OH)}] ₂ Br ₂	0.187	99.0 \pm 0.30	36.93	ND	T
[N _{1,1,16,2(OH)}] ₂ Br ₂	0.182	100 \pm 1.21	0.68	ND	T
[N _{1,1,Bn,2(OH)}] ₂ Br ₂	0.193	97.3 \pm 0.38	3.92	ND	NT
[N _{1,8,2(OH),2(OH)}] ₂ Br ₂	0.196	89.9 \pm 1.60	29.1	NT	NT
[N _{1,10,2(OH),2(OH)}] ₂ Br ₂	0.186	100 \pm 0.65	1.59	NT	NT
[N _{1,12,2(OH),2(OH)}] ₂ Br ₂	0.177	93.8 \pm 2.84	0.61	NT	NT
[N _{6,2(OH),2(OH)2(OH)}] ₂ Br ₂	0.184	93.0 \pm 0.21	41.22	NT	NT
[N _{8,2(OH),2(OH)2(OH)}] ₂ Br ₂	0.175	97.9 \pm 0.74	16.76	VT	NT
[N _{10,2(OH),2(OH)2(OH)}] ₂ Br ₂	0.167	98.2 \pm 1.12	5.21	ND	NT
[N _{12,2(OH),2(OH)2(OH)}] ₂ Br ₂	0.160	100 \pm 2.11	5.22	VT	VT
[N _{Bn,2(OH),2(OH)2(OH)}] ₂ Br ₂	0.157	100 \pm 2.69	11.1	ND	T
tacrine	0.05	61.9 \pm 1.88	0.021	-	-
			0.018		
donepezil	NT	NT	(0.006–0.012)	-	-

^aCompounds from series C were tested at a single dose in each biological assay. ^bCompounds were considered NT, T, or VT when the viability decrease did not attain the IC₅₀ of the compound (less than 50%) or reached 50–80% decrease or was higher than 80%, respectively. “-” not evaluated.

DIL concentration. The STD-NMR experiments were carried out following the protocol previously described by us.⁴¹ Control experiments were accomplished in two ways: (i) sample with the ligand in the absence of AChE [to optimize the frequency for protein saturation (–0.5 ppm) and to ensure that the ligand signals were not affected] and (ii) sample with AChE in the absence of DIL. The STD spectrum of DIL in the absence of AChE shows residual STD response, which was subtracted during the analysis of the STD in the presence of AChE. To determine the epitope mapping of DIL, the STD intensities of each proton were normalized relative to the proton with the highest STD enhancement. In the binding competitions with galanthamine, identical STD-NMR setup was used. All data were processed using TopSpin 3.5 software (Bruker).

3. RESULTS AND DISCUSSION

Monocationic ILs and dicationic DILs were synthesized and cytotoxicity was tested in human normal skin fibroblasts (CRL-1502) and human intestinal adenocarcinoma cells (CaCo-2), before the assessment of the cell viability.

3.1. AChE Inhibition Assay. **3.1.1. Monocationic Cholinium-Based ILs.** Monocationic cholinium-based ILs were synthesized and divided into two series (A and B) and the difference between them is the number of hydroxyethyl groups bound to the positively charged nitrogen (Table 1). To evaluate their potential to inhibit AChE, compounds were tested at 100 μ g/mL in an enzymatic assay with electric eel AChE. Different structural features were investigated for structure–activity relationship studies: the length of the alkyl side chains, the addition of hydroxyethyl groups, and the insertion of double and triple bonds between carbons in the side chains. In series A, we also study the presence of cyclic alkyl side chains, namely, cyclohexyl side chains, and the presence of a morpholine derivative.

3.1.1.1. Alkyl Side-Chain Length. For both series A and B, ILs of different alkyl side-chain lengths were synthesized and tested. Results are shown in Table 3 and clearly demonstrate that lipophilicity has an enormous impact on the induced inhibitory activity. In this sense, the inhibition increased with

the increase of the alkyl side-chain length, and this effect was seen in both series A and B. AChE activity was only gently decreased when the alkyl side chain R was in the range C₂H₅–C₈H₁₇ (series A) or the alkyl side chain R² was in the range C₃H₇–C₆H₁₃ (series B). However, for longer alkyl side-chain lengths, the induced AChE inhibition increased {[N_{1,1,10–16,2(OH)}]₂Br (series A), [N_{0,12–14,2(OH),2(OH)}]₂Br, and [N_{1,10–14,2(OH),2(OH)}]₂Br (series B)}. The best AChE inhibitory activity was observed for compounds [N_{1,1,16,2(OH)}]₂Br (series A) and [N_{1,1,14,2(OH),2(OH)}]₂Br (series B), whose induced inhibition was approximately 100% at the tested dose and determined IC₅₀ values were 5.94 and 7.87 μ M, respectively. In general, for both investigated series, we observed high AChE inhibition from the alkyl side-chain length with 10 or more carbons, which confirmed the well-known side-chain effect tendency.^{23,24}

3.1.1.2. Substitution by an Alkyl Chain by a Hydrogen Atom. Compounds from series B were also synthesized with R¹ equal to H. This change allows the study of the cations with two hydroxyethyl groups, an alkyl side chain and a hydrogen group. This modification of series B enhanced the IL activity to some extent: [N_{0,3,2(OH),2(OH)}]₂Br reduced approximately half of the enzyme activity, whereas [N_{1,3,2(OH),2(OH)}]₂Br induced about 30% inhibition (Table 3). In agreement, and for the longest R² chains, the same general tendency was obtained: at 100 μ g/mL, [N_{0,14,2(OH),2(OH)}]₂Br was able to abrogate almost all the enzyme activity; however, [N_{1,14,2(OH),2(OH)}]₂Br induced about 75% inhibition and determined IC₅₀ values are 11.3 and 7.87 μ M, respectively (Table 3).

3.1.1.3. Addition of Hydroxyethyl Groups. In general, we did not obtain an improvement in activity with the increasing number of hydroxyethyl groups. For instance, data show that [N_{1,1,4,2(OH)}]₂Br, [N_{1,4,2(OH),2(OH)}]₂Br, and [N_{4,2(OH),2(OH),2(OH)}]₂Br led to an inhibition of 64, 66, and 37%, respectively. A decrease in inhibition was also seen for the IL pair [N_{1,1,6,2(OH)}]₂Br and [N_{1,6,2(OH),2(OH)}]₂Br that inhibited the activity of the enzyme by 26% and only 8%, respectively. A decrease in enzymatic inhibition was also demonstrated to some extent when [N_{1,1,10,2(OH)}]₂Br was changed to [N_{1,10,2(OH),2(OH)}]₂Br. We

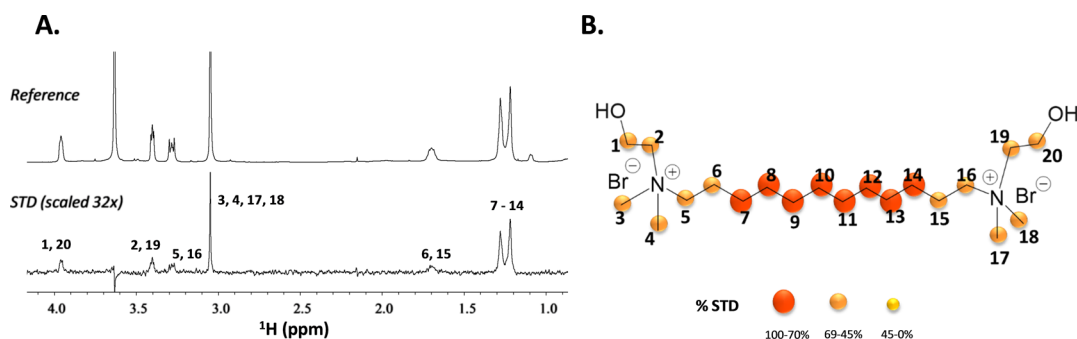


Figure 1. A) STD-NMR binding experiment of $[N_{1,1,12,2(OH)_2}]_2Br_2$ (300 μM) in the presence of AChE (20 μM) at 298 K. The upper spectrum corresponds to the reference spectrum (off-resonance spectrum), and the lower spectrum corresponds to the STD spectrum (scaled 32 \times with respect to the reference). (B) STD-derived epitope mapping of $[N_{1,1,12,2(OH)_2}]_2Br_2$ in the presence of AChE.

may then infer that addition of hydroxyethyl groups does not favor designing of more active ILs, indeed.

3.1.1.4. Insertion of Multiple Covalent Bonds. We also assessed the impact of the insertion of double and triple covalent bonds in the alkyl side chain R (series A) and R¹ and R² (series B). Comparing $[N_{1,1,3,2(OH)}]Br$ with $[N_{1,1,3=2(OH)}]Br$ and $[N_{1,1,3\equiv 2(OH)}]Br$, we realize that the IL-induced AChE inhibition is not significantly affected because the determined inhibition values were 53, 48, and 51%, respectively (Table 3). The same trend occurred with $[N_{1,1,6,2(OH)}]Br$ and $[N_{1,1,6=2(OH)}]Br$ that inhibited the tested enzyme by 26 and 29%, respectively (Table 3). Similar effect was obtained for compounds within series B: $[N_{1,3,2(OH)_2}]Br$, $[N_{1,3=2(OH)_2}]Br$, and $[N_{3=2(OH)_2(OH)_2}]Br$ gently reduced the enzyme activity in about 32, 37, and 21%, respectively (Table 3).

3.1.1.5. Presence of Morpholine and Cyclohexyl in the Cation. In series A, the presence of a cyclohexyl side-chain R ($[N_{1,1,Cycl,2(OH)}]Br$) and the presence of a morpholine derivative ($[N_{1,morf,2(OH)}]Br$) were also evaluated in the enzyme activity. The results showed no significant improvement in the enzyme activity of 31 and 24%, respectively, when compared with the corresponding hexyl side-chain R, $[N_{1,1,6,2(OH)}]Br$ with 26%.

3.1.2. Dicationic Cholinium-Based ILs. Similar to the monocationic cholinium-based ILs, different compounds were produced with differences concerning the length of the alkyl side chains, the number of hydroxyethyl groups, the substitution of CH_2CH_2OH by $CH_2CH_2OCOCH_3$, and the presence or absence of a dibenzyl in the spacer instead of a hydrocarbon chain (see series C–D, Table 2). The DILs were tested for AChE activity as mentioned previously for the monocations, and these compounds exhibited clearly a higher inhibitory activity toward the studied enzyme than the corresponding monocationic cholinium-based ILs (Tables 2 and 4).

3.1.2.1. Alkyl-Linkage Chain Length. As shown in Table 4, the activity of DILs improves with the length of the alkyl-linkage chain. $[N_{1,8,2(OH)_2(OH)}]_2Br_2$, $[N_{1,10,2(OH)_2(OH)}]_2Br_2$, and $[N_{1,12,2(OH)_2(OH)}]_2Br_2$ led to a determined IC_{50} of 29.11, 1.59, and 0.61 μM , respectively. This trend was also observed in the presence of an additional hydroxyethyl: $[N_{8,2(OH)_2(OH)_2(OH)}]_2Br_2$, $[N_{10,2(OH)_2(OH)_2(OH)}]_2Br_2$, and $[N_{12,2(OH)_2(OH)_2(OH)}]_2Br_2$ resulted in an IC_{50} of 16.76, 5.21, and 5.22 μM , respectively.

3.1.2.2. Addition of Hydroxyethyl Groups. As mentioned in the previous subsection, the determined high IC_{50} values

shows that it is necessary higher amounts of $[N_{10,2(OH)_2(OH)_2(OH)}]_2Br_2$ and $[N_{12,2(OH)_2(OH)_2(OH)}]_2Br_2$ than the corresponding $[N_{1,10,2(OH)_2(OH)}]_2Br_2$ and $[N_{1,12,2(OH)_2(OH)}]_2Br_2$ to attain 50% of inhibition. However, the same was not verified for the shorter $[N_{1,8,2(OH)_2(OH)}]_2Br_2$ and $[N_{8,2(OH)_2(OH)_2(OH)}]_2Br_2$ ILs. Additionally, if we compare $[N_{1,1,Bn,2(OH)}]_2Br_2$ and $[N_{Bn,2(OH)_2(OH)_2(OH)}]_2Br_2$, any advantage was due to the addition of another hydroxyethyl group because the determined IC_{50} values are 3.92 and 11.1 μM , respectively (Table 4). As previously demonstrated for the monocationic cholinium-based ILs, the addition of hydroxyethyl groups does not seem to favor the designing of more active ILs.

3.1.2.3. Insertion of Acetyl Groups. In series C, when R is $COCH_3$ instead of H, the IC_{50} is just gently affected increasing from 0.18 to 0.42 μM (Tables 3 and 4), and thus, we conclude that this structural modification does not improve the design of more effective inhibitors.

3.1.2.4. Insertion of Benzyl Groups as Spacers. When the spacer between the cations is two benzyl groups, instead of a hydrocarbon chain, the induced inhibition toward the tested enzyme is reduced: $[N_{1,1,Bn,2(OH)}]_2Br_2$ and $[N_{Bn,2(OH)_2(OH)_2(OH)}]_2Br_2$ produced an IC_{50} of 3.92 and 11.1 μM that are significantly higher than the IC_{50} obtained for $[N_{1,1,12,2(OH)}]_2Br_2$ (0.18 μM) (Tables 3 and 4).

Given these results, we may conclude that the DILs are more promising than the monocationic ILs. Our best results were obtained for the DILs $[N_{1,1,12,2(OH)}]_2Br_2$, $[N_{1,1,12,2(OCOCH_3)}]_2Br_2$, $[N_{1,1,16,2(OH)}]_2Br_2$, and $[N_{1,12,2(OH)_2(OH)}]_2Br_2$ with IC_{50} of 0.18, 0.42, 0.68, and 0.61 μM , with a spacer between the cations of the C₁₂–C₁₆ chain. When we compared the DILs with the corresponding monocationic ILs, the IC_{50} of the DILs is always lower, as observed for the DIL $[N_{1,1,12,2(OH)}]_2Br_2$ with an IC_{50} of 0.18 μM versus the monocationic ILs $[N_{1,1,12,2(OH)}]Br$, $[N_{0,12,2(OH)_2(OH)}]Br$, $[N_{1,12,2(OH)_2(OH)}]Br$ (IC_{50} of 13.81, 32.54, and 23.96 μM) and the DILs $[N_{1,1,16,2(OH)}]_2Br_2$ versus $[N_{1,1,16,2(OH)}]Br$ with an IC_{50} of 0.68 versus 5.94 μM . From our screening of DILs, the best result was obtained for the compound $[N_{1,1,12,2(OH)}]_2Br_2$ with an IC_{50} of 0.18 μM . Possibly, both cations may interact with different binding sites, and the C₁₂ chain seems to be the most suitable length between these two suggested locations. This proposition agrees with the literature, which has shown that both catalytic and PAS sites are important targeted binding sites.¹⁰

3.2. STD-NMR Binding Experiments. STD-NMR is a very popular and robust ligand-based methodology to investigate receptor–ligand interactions in distinct biological

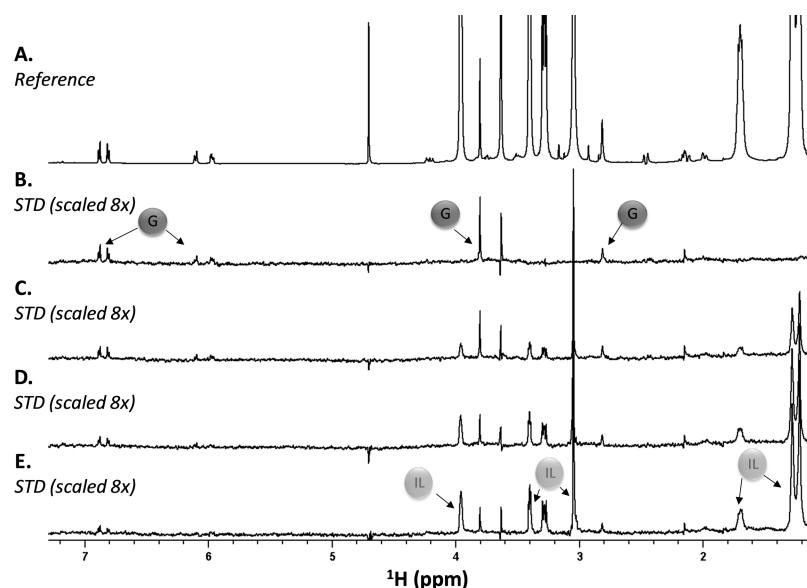


Figure 2. STD competition experiments of AChE/galanthamine at a constant 1:30 M ratio (AChE 10 μM and galanthamine 300 μM) recorded in a 600 MHz spectrometer at 298 K with distinct concentrations of DIL. Proton signals of galanthamine and $[\text{N}_{1,1,12,2(\text{OH})}_2]\text{Br}_2$ are identified with letters G and IL, respectively. (A) Reference spectrum (off-resonance) for the mixture AChE/galanthamine with $[\text{N}_{1,1,12,2(\text{OH})}_2]\text{Br}_2$ 2400 μM . (B) STD spectrum of the mixture AChE/galanthamine without DIL. (C) STD spectrum of the AChE/galanthamine mixture with $[\text{N}_{1,1,12,2(\text{OH})}_2]\text{Br}_2$ 300 μM . (D) STD spectrum of the AChE/galanthamine mixture with $[\text{N}_{1,1,12,2(\text{OH})}_2]\text{Br}_2$ 1200 μM . (E) STD spectrum of the mixture AChE/galanthamine mixture with $[\text{N}_{1,1,12,2(\text{OH})}_2]\text{Br}_2$ 2400 μM .

contexts.^{41,42} STD-NMR allows to deduce ligand binding, as well as, to define which part of the ligand is in closer contact with the receptor, the so-called ligand binding epitope.⁴³(and references cited herein) Indeed, by employing STD-NMR, we were able to determine the interaction between AChE and the most promising DIL, the $[\text{N}_{1,1,12,2(\text{OH})}_2]\text{Br}_2$. This IL is revealed to be the most active inhibitor of AChE activity without affecting the viability of the tested cells.

Figure 1 shows the STD results obtained for the $[\text{N}_{1,1,12,2(\text{OH})}_2]\text{Br}_2$ /AChE mixture. The STD-NMR spectrum clearly shows STD signals corresponding to the DIL in the presence of AChE (Figure 1A). To establish the binding specificity of the system, STD experiments, recorded at different concentrations of AChE, were carried out. The STD signal response clearly increased with the protein concentration providing the specificity of the binding process (Figure S11, Supporting Information). The STD-derived epitope mapping of DIL in the presence of AChE was also deduced (Figure 1B and see Methods and Materials).

According to the STD-derived epitope mapping, all $[\text{N}_{1,1,12,2(\text{OH})}_2]\text{Br}_2$ structure is in closer contact with the protein surface because all protons receive high percentage of saturation from the protein. This result can be explained if the binding site of DIL is deeply located inside the gorge of AChE.

To confirm this hypothesis and to unveil the DIL binding site in AChE, STD-NMR competition binding experiments were performed. These experiments allow to determine if two ligands compete or not for the same binding site of the protein.⁴⁴ Therefore, a ligand with a well-defined binding site and known affinity is normally chosen as a reference. After addition of the study ligand, a reduction of the intensity of the STD signals of the reference ligand will be expected, if both compete for the same binding site of the protein (otherwise allosteric effects take place). However, if the intensity of STD signals of the reference ligand remains unperturbed, the study

ligand and the reference ligand bind at different binding sites of the protein. To determine the binding site of $[\text{N}_{1,1,12,2(\text{OH})}_2]\text{Br}_2$ to AChE, the well-known inhibitor galanthamine was chosen. Galanthamine was chosen because it binds to AChE in the deep gorge active site of AChE with an IC_{50} value of 0.35 μM .⁴⁵ For that purpose, the STD-NMR experiment of the mixture AChE/galanthamine with a molar ratio of 1:30 was first acquired (Figure 2A,B). Further, the intensity variations in the STD spectra of the AChE/galanthamine mixture were monitored by adding three different concentrations of the $[\text{N}_{1,1,12,2(\text{OH})}_2]\text{Br}_2$ (300 μM , 1.2 mM, and 2.4 mM) (Figure 2C–E). After analyzing the STD spectra, it is possible to deduce that $[\text{N}_{1,1,12,2(\text{OH})}_2]\text{Br}_2$ displaces galanthamine from the AChE binding site. A decrease in the STD signal intensity of galanthamine protons occurs after the addition of DIL pointing out that both ligands compete for the same binding site in AChE. In addition, a reverse STD competition binding experiment at a constant AChE/DIL molar ratio with distinct concentrations of galanthamine (300 μM , 1.2 mM, and 2.4 mM) was also carried out (Figure S12, Supporting Information). In agreement, the addition of galanthamine induces a decrease in the intensity of DIL STD signals. Altogether, the STD results highlight that DIL should bind the deep gorge of AChE.

3.3. Molecular Modeling. Finally, to obtain a 3D view of the AChE/DIL complex, we performed in silico molecular docking studies in the active site of AChE, using GOLD 5.1 software.⁴⁶ The coordinates of the enzyme structure were obtained from Protein Data Bank selecting the structure with accession code 4BDT. AChE has its catalytic triad, Ser-His-Glu, located at the bottom of a deep and narrow gorge where the Ser residue acts as a nucleophile to attack the carbonyl groups of substrates or pseudosubstrate inhibitors.⁴⁷ The docked pose for the most active compound $[\text{N}_{1,1,12,2(\text{OH})}_2]\text{Br}_2$ shows that, as anticipated by the STD-derived epitope map, the dicationic C_{12} inhibitor is very well accommodated in the

enzyme gorge (Figure 3). The proposed binding mode is also in agreement with the STD competition binding experiments

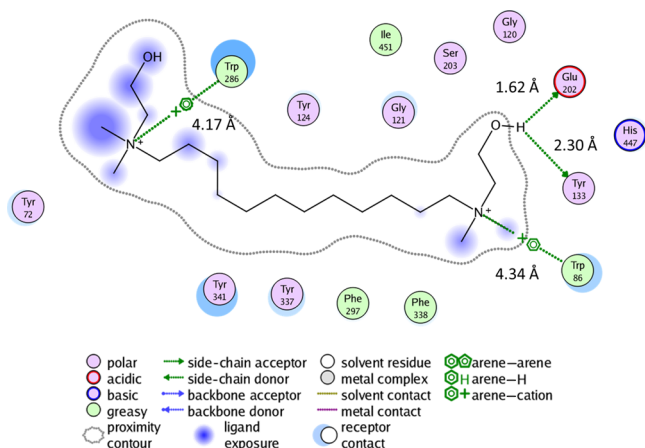


Figure 3. GOLD docking pose interaction diagram for $[N_{1,1,12,2(OH)}]_2Br_2$ in AChE gorge using MOE 2012.10 software.⁴⁰

using galanthamine as a reference ligand. According to our model, DIL interacts with both PAS and catalytic sites of AChE. In particular, one of the quaternary amines sits well in the catalytic site where the cation- π interaction with Trp86 is observed, and the hydroxyl establishes an H-bond with Glu202, blocking the action of the catalytic triad, whereas the other quaternary amine, which is 12 carbons away, sits on the entrance of the gorge where the cation- π interaction with Trp286 is observed. The presence of interactions in both PAS and catalytic sites seems mandatory for the recognition of DILs as AChE inhibitors.

3.4. Toxicity Evaluation on Human Cell Lines. Tested ILs were evaluated on human cell lines CRL-1502 and CaCo-2. Cell monolayers were grown and exposed to a single dose (1 mM) of the compounds for a period of 24 h before the assessment of cell monolayer viability.

3.4.1. Monocationic Cholinium-Based ILs. **3.4.1.1. Alkyl Side-Chain Length.** As expected, monocationic cholinium-based ILs induced high levels of cytotoxicity when the alkyl side chain R (series A) or R² (series B) was one of the following chains: C₁₀H₂₁, C₁₂H₂₃, C₁₄H₂₉, and C₁₆H₃₃ (Table 3). This effect is already known in the literature.^{48,49}

3.4.1.2. Substitution by an Alkyl Chain by a Hydrogen Atom. Data are not very clear about this structural modification; however, it seems that there is some decrease in CaCo-2 toxicity when R¹ in $[N_{1,12,2(OH),2(OH)}]Br$ is substituted by a hydrogen atom— $[N_{0,12,2(OH),2(OH)}]Br$ (Table 3). However, when the length of the alkyl side chain R² is increased to C₁₄H₂₇ (R¹ equal to H and CH₃), we obtain high cytotoxicity in CRL-1502 cells, meaning that the effect seen previously is possibly less and less evident when the length of the side-chain R² increases (Table 3).

3.4.1.3. Addition of Hydroxyethyl Groups. The effect of this modification is more noticeable. As shown in Table 3, we did not obtain a significant toxicity for either $[N_{1,1,4,2(OH)}]Br$ or $[N_{1,4,2(OH),2(OH)}]Br$, independently of the tested cell model; however, when $[N_{4,2(OH),2(OH),2(OH)}]Br$ was tested, a great cytotoxicity in CaCo-2 monolayer was observed, despite having no significant effect on the other cell line. Following the same trend, any significant toxicity was quantified for either $[N_{1,1,6,2(OH)}]Br$ or $[N_{1,6,2(OH),2(OH)}]Br$, but $[N_{6,2(OH),2(OH),2(OH)}]Br$

proved to be cytotoxic to Caco-2 cells (data not available for CRL-1502 cells). Considering this, it is best to use less hydroxyethyl groups when designing biologically active ILs because it may potentially increase the cytotoxicity without conferring any advantage in terms of activity toward AChE, as mentioned previously.

3.4.1.4. Insertion of Multiple Covalent Bonds. Concerning the insertion of multiple covalent bonds, we did not obtain any detectable effect on the viability of the tested cell models (Table 3).

3.4.1.5. Presence of Morpholine and Cyclohexyl in the Cation. We did not obtain any detectable effect on monolayer viability concerning the two cell models used in this study.

3.4.2. Dicationic Cholinium-Based ILs. Similar to ILs from series A and B, the impact of dicationic cholinium-based ILs on the cell monolayer was also assessed in normal skin fibroblasts and colorectal adenocarcinoma epithelial cells.

3.4.2.1. Alkyl-Linkage Chain Length. In agreement with other works in the literature and with the data obtained for the monocationic cholinium-based ILs, the cytotoxicity was enhanced with the length of the alkyl-linkage chain (Table 4).³³ Another important conclusion is that DILs are less cytotoxic than the corresponding monocationic ILs. For instance, $[N_{1,12,2(OH)}]Br$ was very cytotoxic for CaCo-2 cells, whereas $[N_{1,12,2(OH)}]_2Br_2$ did not significantly affect this model, and $[N_{1,14,2(OH)}]Br$ induced a great cytotoxicity in CaCo-2 cells, but the corresponding $[N_{1,14,2(OH)}]_2Br_2$ was less deleterious (Table 4). This is in accordance with the literature.²⁸

3.4.2.2. Addition of Hydroxyethyl Groups. As seen before for the monocationic ILs, the addition of hydroxyethyl groups is prone to induce cytotoxicity as is the case of $[N_{1,12,2(OH),2(OH)}]_2Br_2$ and $[N_{12,2(OH),2(OH),2(OH)}]_2Br_2$, where the first did not induce a significant decrease in viability, independently of the cell line. However, the second was very cytotoxic for both models (Table 4). This is in agreement with the data obtained for the monocationic cholinium-based ILs. Additionally, e Silva and co-workers have also published that dicationic cholinium-based IL toxicity increased on the luminescent bacteria *Vibrio fischeri* with the addition of more hydroxyethyl groups.³³ As seen from the biological data collected from the anti-acetylcholinesterase assay, the presence of hydroxyethyl groups does not favor the biological activity of the studied ILs and thus, we conclude that -CH₂CH₂OH chains are not beneficial to attain our purposes.

3.4.2.3. Insertion of Acetyl Groups. The protection of the hydroxyl group with an acetyl group did not produce detectable difference on the toxicological results (Table 4).

3.4.2.4. Insertion of Benzyl Groups as Spacers. Similarly, the introduction of two benzyl groups in the linkage did not seem to produce detectable difference on the toxicological results (Table 4).

4. CONCLUSIONS

The dicationic cholinium-based ILs are better AChE inhibitors than the corresponding monocationic analogue. In addition, DILs with the alkyl linkage of C₁₂–C₁₆ present the most promising AChE inhibition results. The DIL $[N_{1,1,12,2(OH)}]_2Br_2$ shows an IC₅₀ of 0.18 μ M without affecting the viability of the tested cells. To understand the AChE inhibition by $[N_{1,1,12,2(OH)}]_2Br_2$, STD-NMR binding experiments and in silico molecular docking studies were performed. STD-NMR clearly demonstrates that $[N_{1,1,12,2(OH)}]_2Br_2$ competes with

galanthamine for the same binding site of AChE and binds into the deep gorge active site of AChE. In accordance, molecular docking shows that $[N_{1,1,12,2(OH)}]_2Br_2$ establishes key interactions in both peripheral and catalytic sites of AChE gorge. In this perspective, our study provides a chemical platform for the rational design of choline-based ILs as potent AChE inhibitors.

■ ASSOCIATED CONTENT

📄 Supporting Information

The Supporting Information is available free of charge on the ACS Publications website at DOI: 10.1021/acsomega.8b02347.

General procedure for the synthesis of the quaternary ammonium salts—series A; general synthesis of quaternary ammonium salts—series B; general synthesis of bis-quaternary ammonium salts—series C and series D; synthesis of a bis-quaternary ammonium salt—series C; 1H NMR and ^{13}C NMR spectra; and STD-NMR studies (PDF)

■ AUTHOR INFORMATION

Corresponding Authors

*E-mail: filipasiopa@ff.ulisboa.pt (F.S.).

*E-mail: patricia.rijo@ulusofona.pt (P.R.).

ORCID

Filipa Marcelo: 0000-0001-5049-8511

Carlos A. M. Afonso: 0000-0002-7284-5948

Patrícia Rijo: 0000-0001-7992-8343

Notes

The authors declare no competing financial interest.

■ ACKNOWLEDGMENTS

The authors thank the financial support of FCT (Fundação para a Ciência e Tecnologia-Portugal) through the post-doctoral grants (SFRH/BPD/73822/2010 and SFRH/BPD/88666/2012) and projects (UID/DTP/04138/2013, UID/DTP/04567/2016, and COMPETE Programme: SAICTPAC/0019/2015). F.M. thanks the FCT for IF investigator project IF/00780/2015. The NMR spectrometers are part of the National NMR Network (PTNMR) and are partially supported by Infrastructure Project no. 022161 (cofinanced by FEDER through COMPETE 2020, POCI and PORL and FCT through PIDDAC). The authors would like to acknowledge networking contribution by the COST Action CM1407 “Challenging organic synthesis inspired by nature—from natural products chemistry to drug discovery”.

■ REFERENCES

- (1) Quinn, D. M. Acetylcholinesterase: enzyme structure, reaction dynamics, and virtual transition states. *Chem. Rev.* **1987**, *87*, 955–979.
- (2) Meshorer, E.; Soreq, H. Virtues and woes of AChE alternative splicing in stress-related neuropathologies. *Trends Neurosci.* **2006**, *29*, 216–224.
- (3) Singh, M.; Kaur, M.; Kukreja, H.; Chugh, R.; Silakari, O.; Singh, D. Acetylcholinesterase inhibitors as Alzheimer therapy: From nerve toxins to neuroprotection. *Eur. J. Med. Chem.* **2013**, *70*, 165–188.
- (4) Sussman, J.; Harel, M.; Frolow, F.; Oefner, C.; Goldman, A.; Toker, L.; Silman, I. Atomic structure of acetylcholinesterase from Torpedo californica: a prototypic acetylcholine-binding protein. *Science* **1991**, *253*, 872–879.
- (5) Conejo-García, A.; Pisani, L.; del Carmen Núñez, M.; Catto, M.; Nicolotti, O.; Leonetti, F.; Campos, J. M.; Gallo, M. A.; Espinosa, A.; Carotti, A. Homodimeric Bis-Quaternary Heterocyclic Ammonium

Salts as Potent Acetyl- and Butyrylcholinesterase Inhibitors: A Systematic Investigation of the Influence of Linker and Cationic Heads over Affinity and Selectivity. *J. Med. Chem.* **2011**, *54*, 2627–2645.

(6) Wyman, I. W.; Macartney, D. H. Host–Guest Complexes and Pseudorotaxanes of Cucurbit[7]uril with Acetylcholinesterase Inhibitors. *J. Org. Chem.* **2009**, *74*, 8031–8038.

(7) Yu, Q.-s.; Holloway, H. W.; Utsuki, T.; Brossi, A.; Greig, N. H. Synthesis of Novel Phenserine-Based-Selective Inhibitors of Butyrylcholinesterase for Alzheimer's Disease. *J. Med. Chem.* **1999**, *42*, 1855–1861.

(8) Schwarz, S.; Loesche, A.; Lucas, S. D.; Sommerwerk, S.; Serbian, I.; Siewert, B.; Pianowski, E.; Csuk, R. Converting maslinic acid into an effective inhibitor of acylcholinesterases. *Eur. J. Med. Chem.* **2015**, *103*, 438–445.

(9) Kryger, G.; Silman, I.; Sussman, J. L. Structure of acetylcholinesterase complexed with E2020 (Aricept): implications for the design of new anti-Alzheimer drugs. *Structure* **1999**, *7*, 297–307.

(10) Stavrakov, G.; Philipova, I.; Zheleva, D.; Atanasova, M.; Konstantinov, S.; Doytchinova, I. Docking-based Design of Galantamine Derivatives with Dual-site Binding to Acetylcholinesterase. *Mol. Inf.* **2016**, *35*, 278–285.

(11) Komloova, M.; Horova, A.; Hrabina, M.; Jun, D.; Dolezal, M.; Vinsova, J.; Kuca, K.; Musilek, K. Preparation, in vitro evaluation and molecular modelling of pyridinium-quinolinium/isoquinolinium non-symmetrical bisquaternary cholinesterase inhibitors. *Bioorg. Med. Chem. Lett.* **2013**, *23*, 6663–6666.

(12) Schwarz, S.; Lucas, S. D.; Sommerwerk, S.; Csuk, R. Amine derivatives of glycyrrhetic acid as potential inhibitors of cholinesterases. *Bioorg. Med. Chem.* **2014**, *22*, 3370–3378.

(13) Komloova, M.; Musilek, K.; Dolezal, M.; Gunn-Moore, F.; Kuca, K. Structure-Activity Relationship of Quaternary Acetylcholinesterase Inhibitors - Outlook for Early Myasthenia Gravis Treatment. *Curr. Med. Chem.* **2010**, *17*, 1810–1824.

(14) Li, J.-C.; Zhang, J.; Rodrigues, M. C.; Ding, D.-J.; Longo, J. P. F.; Azevedo, R. B.; Muehlmann, L. A.; Jiang, C.-S. Synthesis and evaluation of novel 1,2,3-triazole-based acetylcholinesterase inhibitors with neuroprotective activity. *Bioorg. Med. Chem. Lett.* **2016**, *26*, 3881–3885.

(15) Parveen, M.; Aslam, A.; Nami, S. A. A.; Malla, A. M.; Alam, M.; Lee, D.-U.; Rehman, S.; Pereira Silva, P. S.; Ramos Silva, M. Potent acetylcholinesterase inhibitors: Synthesis, biological assay and docking study of nitro acridone derivatives. *J. Photochem. Photobiol., B* **2016**, *161*, 304–311.

(16) Musilek, K.; Komloova, M.; Zavadova, V.; Holas, O.; Hrabina, M.; Pohanka, M.; Dohnal, V.; Nachon, F.; Dolezal, M.; Kuca, K.; Jung, Y.-S. Preparation and in vitro screening of symmetrical bispyridinium cholinesterase inhibitors bearing different connecting linkage-initial study for Myasthenia gravis implications. *Bioorg. Med. Chem. Lett.* **2010**, *20*, 1763–1766.

(17) Komloova, M.; Musilek, K.; Horova, A.; Holas, O.; Dohnal, V.; Gunn-Moore, F.; Kuca, K. Preparation, in vitro screening and molecular modelling of symmetrical bis-quinolinium cholinesterase inhibitors-implications for early Myasthenia gravis treatment. *Bioorg. Med. Chem. Lett.* **2011**, *21*, 2505–2509.

(18) Musilek, K.; Komloova, M.; Holas, O.; Hrabina, M.; Pohanka, M.; Dohnal, V.; Nachon, F.; Dolezal, M.; Kuca, K. Preparation and in vitro screening of symmetrical bis-isoquinolinium cholinesterase inhibitors bearing various connecting linkage - Implications for early Myasthenia gravis treatment. *Eur. J. Med. Chem.* **2011**, *46*, 811–818.

(19) Bharate, S. B.; Guo, L.; Reeves, T. E.; Cerasoli, D. M.; Thompson, C. M. Bisquaternary pyridinium oximes: Comparison of in vitro reactivation potency of compounds bearing aliphatic linkers and heteroaromatic linkers for paraoxon-inhibited electric eel and recombinant human acetylcholinesterase. *Bioorg. Med. Chem.* **2010**, *18*, 787–794.

- (20) Srinivas Rao, C.; Venkateswarlu, V.; Achaiah, G. Quaternary salts of 4,3' and 4,4' bis-pyridinium monooximes. Part 2: Synthesis and biological activity. *Bioorg. Med. Chem. Lett.* **2006**, *16*, 2134–2138.
- (21) Musilek, K.; Pavlikova, R.; Marek, J.; Komloova, M.; Holas, O.; Hrabnova, M.; Pohanka, M.; Dohnal, V.; Dolezal, M.; Gunn-Moore, F.; Kuca, K. The preparation, in vitro screening and molecular docking of symmetrical bisquaternary cholinesterase inhibitors containing a but-(2E)-en-1,4-diyl connecting linkage. *J. Enzyme Inhib. Med. Chem.* **2011**, *26*, 245–253.
- (22) Harel, M.; Schalk, I.; Ehret-Sabatier, L.; Bouet, F.; Goeldner, M.; Hirth, C.; Axelsen, P. H.; Silman, I.; Sussman, J. L. Quaternary ligand binding to aromatic residues in the active-site gorge of acetylcholinesterase. *Proc. Natl. Acad. Sci. U.S.A.* **1993**, *90*, 9031–9035.
- (23) Arning, J.; Stolte, S.; Bösch, A.; Stock, F.; Pitner, W.-R.; Welz-Biermann, U.; Jastorff, B.; Ranke, J. Qualitative and quantitative structure activity relationships for the inhibitory effects of cationic head groups, functionalised side chains and anions of ionic liquids on acetylcholinesterase. *Green Chem.* **2008**, *10*, 47–58.
- (24) Stock, F.; Hoffmann, J.; Ranke, J.; Störmann, R.; Ondruschka, B.; Jastorff, B. Effects of ionic liquids on the acetylcholinesterase - a structure-activity relationship consideration. *Green Chem.* **2004**, *6*, 286–290.
- (25) Basant, N.; Gupta, S.; Singh, K. P. Predicting acetyl cholinesterase enzyme inhibition potential of ionic liquids using machine learning approaches: An aid to green chemicals designing. *J. Mol. Liq.* **2015**, *209*, 404–412.
- (26) Luo, Y.-R.; Wang, S.-H.; Yun, M.-X.; Li, X.-Y.; Wang, J.-J.; Sun, Z.-J. The toxic effects of ionic liquids on the activities of acetylcholinesterase and cellulase in earthworms. *Chemosphere* **2009**, *77*, 313–318.
- (27) Das, R. N.; Roy, K. Predictive in silico Modeling of Ionic Liquids toward Inhibition of the Acetyl Cholinesterase Enzyme of *Electrophorus electricus*: A Predictive Toxicology Approach. *Ind. Eng. Chem. Res.* **2014**, *53*, 1020–1032.
- (28) Steudte, S.; Bemowsky, S.; Mahrova, M.; Bottin-Weber, U.; Tojo-Suarez, E.; Stepnowski, P.; Stolte, S. Toxicity and biodegradability of dicationic ionic liquids. *RSC Adv.* **2014**, *4*, 5198–5205.
- (29) Kaur, J.; Zhang, M. Q. Molecular Modelling and QSAR of Reversible Acetylcholinesterase Inhibitors. *Curr. Med. Chem.* **2000**, *7*, 273–294.
- (30) Pernak, J.; Syguda, A.; Mirska, I.; Pernak, A.; Nawrot, J.; Pradzyńska, A.; Griffin, S. T.; Rogers, R. D. Choline-derivative-based ionic liquids. *Chem.—Eur. J.* **2007**, *13*, 6817–6827.
- (31) Zeisel, S. H.; da Costa, K.-A. Choline: an essential nutrient for public health. *Nutr. Rev.* **2009**, *67*, 615–623.
- (32) Yue, H.; Waldeck, D. H.; Schrock, K.; Kirby, D.; Knorr, K.; Switzer, S.; Rosmus, J.; Clark, R. A. Multiple Sites for Electron Tunneling between Cytochrome c and Mixed Self-Assembled Monolayers. *J. Phys. Chem. C* **2008**, *112*, 2514–2521.
- (33) e Silva, F. A.; Siopa, F.; Figueiredo, B. F. H. T.; Gonçalves, A. M. M.; Pereira, J. L.; Gonçalves, F.; Coutinho, J. A. P.; Afonso, C. A. M.; Ventura, S. P. M. Sustainable design for environment-friendly mono and dicationic cholinium-based ionic liquids. *Ecotoxicol. Environ. Saf.* **2014**, *108*, 302–310.
- (34) Hartmann, D. O.; Shimizu, K.; Siopa, F.; Cristina Leitão, M.; Afonso, C. A. M.; Canongia Lopes, J. N.; Silva Pereira, C. Plasma membrane permeabilisation by ionic liquids: a matter of charge. *Green Chem.* **2015**, *17*, 4587–4598.
- (35) Calas, M.; Cordina, G.; Bompard, J.; Ben Bari, M.; Jei, T.; Ancelin, M. L.; Vial, H. Antimalarial Activity of Molecules Interfering with *Plasmodium falciparum* Phospholipid Metabolism. Structure–Activity Relationship Analysis. *J. Med. Chem.* **1997**, *40*, 3557–3566.
- (36) Koufaki, M.; Polychroniou, V.; Calogeropoulou, T.; Tsotinis, A.; Drees, M.; Fiebig, H. H.; LeClerc, S.; Hendriks, H. R.; Makriyannis, A. Alkyl and alkoxyethyl antineoplastic phospholipids. *J. Med. Chem.* **1996**, *39*, 2609–2614.
- (37) Mishra, B. K.; Mukherjee, P.; Dash, S.; Patel, S.; Pati, H. N. Alkylation of Ethanolamines: An Approach to a Novel Class of Functional Surfactants. *Synth. Commun.* **2009**, *39*, 2529–2539.
- (38) Kubínová, R.; Pořízková, R.; Navrátilová, A.; Farsa, O.; Hanáková, Z.; Bačinská, A.; Čížek, A.; Valentová, M. Antimicrobial and enzyme inhibitory activities of the constituents of *Plectranthus madagascariensis* (Pers.) Benth. *J. Enzyme Inhib. Med. Chem.* **2014**, *29*, 749–752.
- (39) Rijo, P.; Falé, P. L.; Serralheiro, M. L.; Simões, M. F.; Gomes, A.; Reis, C. Optimization of medicinal plant extraction methods and their encapsulation through extrusion technology. *Measurement* **2014**, *58*, 249–255.
- (40) MOE, Molecular Operating Environment Chemical Computing Group: Montreal, Canada, 2012 www.chemcomp.com.
- (41) Marcelo, F.; Garcia-Martin, F.; Matsushita, T.; Sardinha, J.; Coelho, H.; Oude-Vrielink, A.; Koller, C.; André, S.; Cabrita, E. J.; Gabius, H.-J.; Nishimura, S.-I.; Jiménez-Barbero, J.; Cañada, F. J. Delineating Binding Modes of Gal/GalNAc and Structural Elements of the Molecular Recognition of Tumor-Associated Mucin Glycopeptides by the Human Macrophage Galactose-Type Lectin. *Chem.—Eur. J.* **2014**, *20*, 16147–16155.
- (42) Viegas, A.; Manso, J.; Corvo, M. C.; Marques, M. M. B.; Cabrita, E. J. Binding of Ibuprofen, Ketorolac, and Diclofenac to COX-1 and COX-2 Studied by Saturation Transfer Difference NMR. *J. Med. Chem.* **2011**, *54*, 8555–8562.
- (43) Meyer, B.; Peters, T. NMR Spectroscopy Techniques for Screening and Identifying Ligand Binding to Protein Receptors. *Angew. Chem., Int. Ed.* **2003**, *42*, 864–890.
- (44) Wang, Y.-S.; Liu, D.; Wyss, D. F. Competition STD NMR for the detection of high-affinity ligands and NMR-based screening. *Magn. Reson. Chem.* **2004**, *42*, 485–489.
- (45) Greenblatt, H. M.; Kryger, G.; Lewis, T.; Silman, I.; Sussman, J. L. Structure of acetylcholinesterase complexed with (–)-galanthamine at 2.3 Å resolution. *FEBS Lett.* **1999**, *463*, 321–326.
- (46) GOLD Cambridge Crystallographic Data Centre: Cambridge, U.K. <https://www.ccdc.cam.ac.uk/solutions/csd-discovery/components/gold/> (accessed March 2018).
- (47) Chiou, S.-Y.; Huang, C.-F.; Hwang, M.-T.; Lin, G. Comparison of active sites of butyrylcholinesterase and acetylcholinesterase based on inhibition by geometric isomers of benzene-di-N-substituted carbamates. *J. Biochem. Mol. Toxicol.* **2009**, *23*, 303–308.
- (48) Frade, R. F. M.; Rosatella, A. A.; Marques, C. S.; Branco, L. C.; Kulkarni, P. S.; Mateus, N. M. M.; Afonso, C. A. M.; Duarte, C. M. M. Toxicological evaluation on human colon carcinoma cell line (CaCo-2) of ionic liquids based on imidazolium, guanidinium, ammonium, phosphonium, pyridinium and pyrrolidinium cations. *Green Chem.* **2009**, *11*, 1660–1665.
- (49) Frade, R. F. M.; Matias, A.; Branco, L. C.; Afonso, C. A. M.; Duarte, C. M. M. Effect of ionic liquids on human colon carcinoma HT-29 and CaCo-2 cell lines. *Green Chem.* **2007**, *9*, 873–877.